Metal Valence and Geometry: Synthesis, Structure and Solution Behaviour of the Isomers of $[Os(S_2CNEt_2)_2(PPh_3)_2]^{0,+}$†

Amitava Pramanik, Nilkamal Bag and Animesh Chakravorty*
Department of Inorganic Chemistry, Indian Association for the Cultivation of Science, Calcutta 700 032, India

The reaction of $[Os(PPh_3)_3Br_2]$ with $Na(S_2CNEt_2)$ affords *cis*-$[OsL_2(PPh_3)_2]$ (L = S_2CNEt_2) from which *trans*-$[OsL_2(PPh_3)_2]PF_6$ is isolated *via* cerium(IV) oxidation. Reduction of the latter complex by hydrazine hydrate furnishes *trans*-$[OsL_2(PPh_3)_2]$. The X-ray structures of all the three complexes have been determined and their spectra and magnetic properties are reported. Solution equilibrium data show that the metal oxidation states strongly differentiate the isomeric co-ordination spheres—the more stable geometry is *cis* for the bivalent and *trans* for the trivalent metal. The metastable *trans*-bivalent complex (d^6) can still be isolated because isomerisation is slow but the *cis*-trivalent complex (d^5) isomerises rapidly and could not be isolated. Variable-temperature isomerisation rates, activation parameters and metal reduction potentials [$E_{\frac{1}{2}}(cis) > E_{\frac{1}{2}}(trans)$] of the isomers are reported. There is a progressive decrease in the Os–P bond length in going from *trans*-$[OsL_2(PPh_3)_2]PF_6$ to *trans*-$[OsL_2(PPh_3)_2]$ to *cis*-$[OsL_2(PPh_3)_2]$, the net change being a remarkable 0.15 Å. This correlates with the $5d_\pi$–$3d_\pi$ back-bonding order *cis*-$[OsL_2(PPh_3)_2]$ > *trans*-$[OsL_2(PPh_3)_2]$ ≫ *trans*-$[OsL_2(PPh_3)_2]PF_6$. In *cis*-$[OsL_2(PPh_3)_2]$, $PPh_3 \cdots PPh_3$ steric repulsion is present but it is more than offset by the strong back-bonding. In *trans*-$[OsL_2(PPh_3)_2]$ the steric factor is absent but the back-bonding is also weaker. In equilibrated solution both the isomers are present but the *cis* form predominates (85%). For the very weakly back-bonding trivalent metal, the steric factor becomes strongly controlling and in solutions very little of the *cis* isomer is present at equilibrium (≈0.002%).

The varied response of co-ordination spheres to changes in the primary valence of the ligated metal centre is of fundamental importance in inorganic redox chemistry.[1,2] An example is geometrical isomerisation[3–9] implying selective binding of different oxidation states by isomeric environments. Our interest lies in probing the origin of such selectivity in terms of experimentally determined bond parameters of the isomers. The prerequisite for this purpose is to have systems where all or most of the possible combinations of geometry and valence can be isolated and structurally characterised. Herein we describe the case of the dithiocarbamate–phosphine system **1** in which the OsS_4P_2 co-ordination sphere can span two geometries (*cis* and *trans*) and two metal oxidation states (+2 and +3). Of the four possible geometry-valence combinations, all except the *cis*-trivalent complex have been isolated. Isomer selectivity of oxidation states is scrutinised in the light of X-ray structures. Equilibrium constants, interconversion rates and reduction potentials of isomers are recorded.

Results and Discussion

Synthesis and Characterisation of Isomers.—The system **1** will be abbreviated as $[OsL_2(PPh_3)_2]^{0,+}$ (L = S_2CNEt_2) where 0 and + charges correspond respectively to the bi- and tri-valent states of the metal. The reaction of $[Os(PPh_3)_3Br_2]$ with NaL in boiling ethanol affords *cis*-$[OsL_2(PPh_3)_2]$ as a yellow crystalline solid. Upon oxidation of this complex in dichloromethane–acetonitrile solution with aqueous $[NH_4]_4[Ce(SO_4)_4]\cdot 2H_2O$, green *trans*-$[OsL_2(PPh_3)_2]^+$ is formed which is isolated as the PF_6^- salt. The *cis*-$[OsL_2(PPh_3)_2]^+$ isomer is formed as an intermediate, but it could not be isolated due to fast isomerisation (see below). When *trans*-$[OsL_2(PPh_3)_2]PF_6$ is reduced by hydrazine hydrate in acetonitrile solution in the cold (to prevent isomerisation of product) orange-yellow *trans*-$[OsL_2(PPh_3)_2]$ separates. The yield in each of the above steps is >90%. The complex *cis*-$[OsL_2(PPh_3)_2]$ has been reported earlier as a low-yield product of the reaction of NaL with hydrido(trifluoroacetato)tetrakis(triphenylphosphine) osmium.[10]

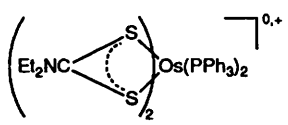

1

Elemental analyses and electronic spectral data of the complexes are listed in Table 1. The 1:1 electrolytic (Λ = 137 Ω^{-1} cm^2 mol^{-1}) *trans*-$[OsL_2(PPh_3)_2]PF_6$ complex is paramagnetic ($S = \frac{1}{2}$, μ_{eff}, 1.87) and displays a rhombic EPR spectrum in frozen solution (Fig. 1) in gross accord with the C_i symmetry of the OsS_4P_2 sphere as revealed by X-ray structure determination, see below. Analysis of the spectrum with the help of *g*-tensor theory[11,12] for low-spin d^5 ions (t_2^5) affords the axial (Δ) and rhombic (V) distortion parameters of magnitude 7500 and 1900 cm^{-1} [the spin-orbit coupling constant of osmium(III) is taken[13] as 3000 cm^{-1}]. Two transitions among the three t_2 Kramers doublets are predicted to lie near 7000 cm^{-1} (ν_1) and 10 000 cm^{-1} (ν_2). The electronic spectrum of the complex is displayed in Fig. 1. A relatively weak band observed at 1300 nm (7460 cm^{-1}) is assigned to ν_1. The tail of the strong band at 635 nm probably obscures the ν_2 band.

Structures.—The structures of all the three complexes have been determined. Molecular views and atom labelling schemes are shown in Figs. 2–4. Selected bond distances and angles are listed in Tables 2 and 3. The bond parameters (C–S, C–N

† *Supplementary data available:* see Instructions for Authors, *J. Chem. Soc., Dalton Trans.*, 1993, Issue 1, pp. xxiii–xxviii.

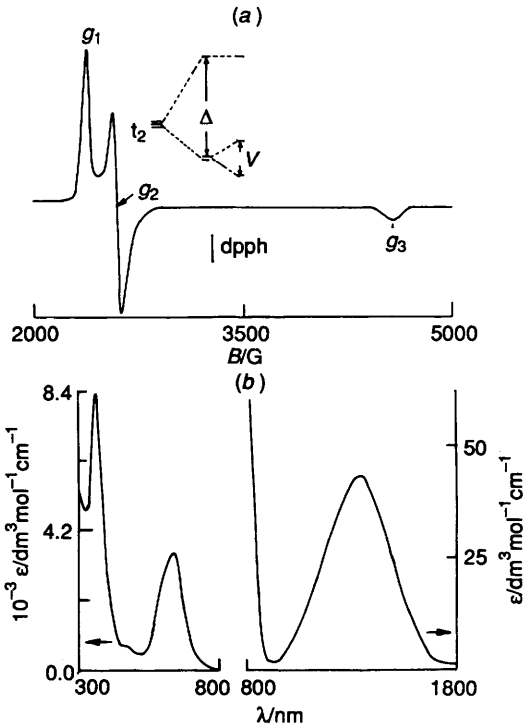

Fig. 1 (*a*) X-Band EPR spectrum and t_2 splittings of *trans*-$[OsL_2(PPh_3)_2]PF_6$ in dichloromethane–toluene (1:1) glass (77 K): $g_1 = 2.7645$, $g_2 = 2.5249$, $g_3 = 1.4368$, $\Delta = 7530$ cm^{-1}, $V = 1930$ cm^{-1}, G = 10^{-4} T. (*b*) Electronic spectrum of *trans*-$[OsL_2(PPh_3)_2]PF_6$ in dichloromethane at 298 K

lengths, S–C–S angles *etc.*) within the diethyldithiocarbamate ligand of the present complexes generally agree with those reported for other diethyldithiocarbamate complexes.[14–16]

In the *cis*-$[OsL_2(PPh_3)_2]$ complex there are two independent molecules in the asymmetric unit. These are very similar to each other except for the conformation of the NEt_2 fragments. In molecule 1 the terminal methyl groups adopt *anti* configurations

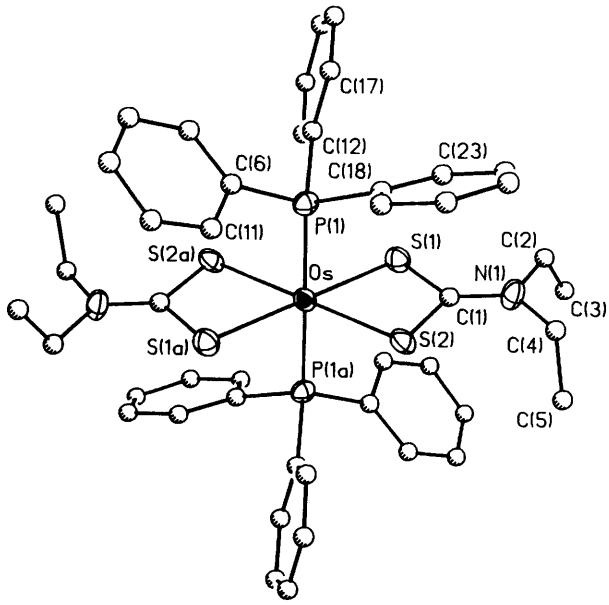

Fig. 3 Perspective view and atom labelling scheme for *trans*-$[OsL_2(PPh_3)_2]$

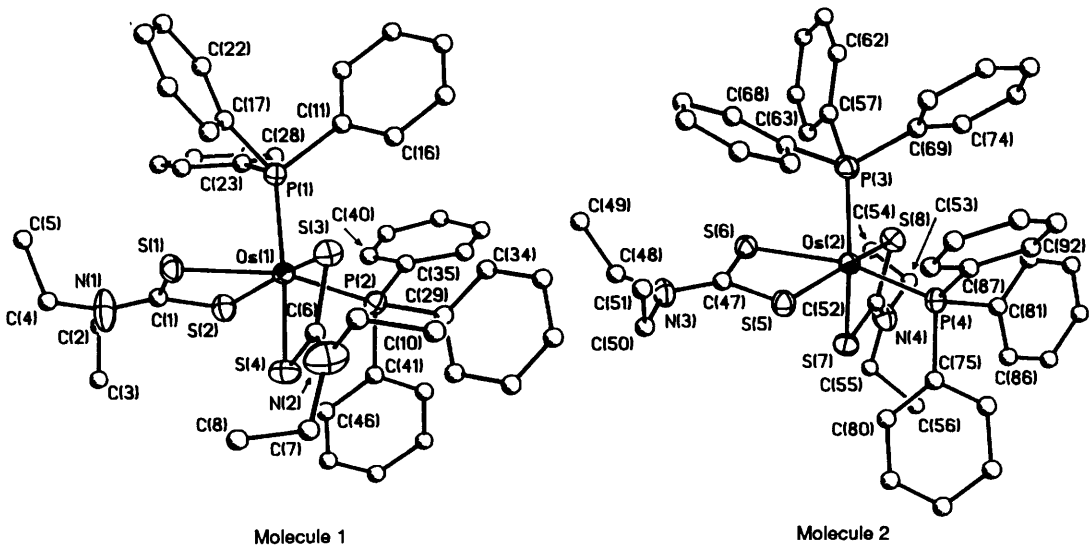

Fig. 2 Perspective view and atom labelling scheme for the two independent molecules of *cis*-$[OsL_2(PPh_3)_2]$

Table 1 Analytical[a] and electronic spectral data[b]

Compound	Analysis (%) C	H	N	UV/VIS and NIR spectral data, λ_{max}/nm (ε/dm^3 mol^{-1} cm^{-1})
cis-$[OsL_2(PPh_3)_2]$	54.50 (54.60)	4.95 (5.00)	2.75 (2.75)	350 (11 880), 260 (sh) (20 700)
trans-$[OsL_2(PPh_3)_2]$	54.60 (54.60)	4.95 (5.00)	2.80 (2.75)	475 (1535), 380 (7410), 260 (sh) (32 105)
trans-$[OsL_2(PPh_3)_2]PF_6$	47.70 (47.75)	4.35 (4.30)	2.40 (2.40)	1340 (44), 635 (4030), 475 (sh) (800), 360 (8320), 270 (25 600)

[a] Calculated values are in parentheses. [b] In dichloromethane at 298 K.

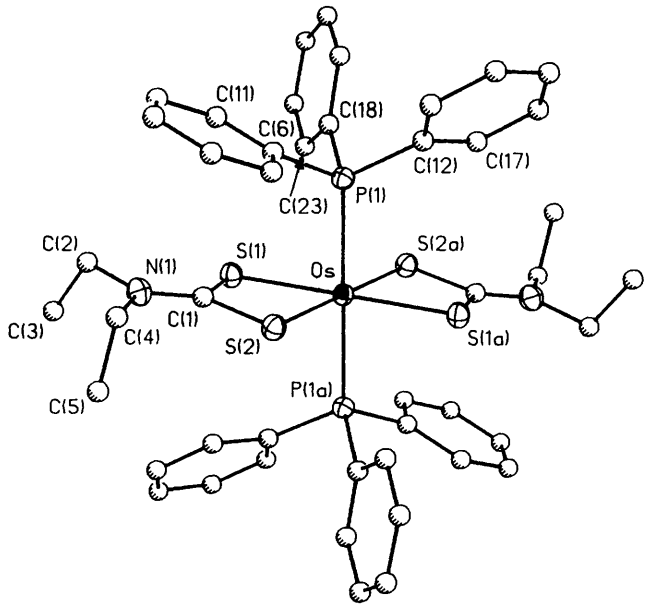

Fig. 4 Perspective view and atom labelling scheme for the cation of *trans*-$[OsL_2(PPh_3)_2]PF_6$

Table 2 Selected bond distances (Å) and angles (°) for *cis*-$[OsL_2(PPh_3)_2]$

Molecule 1		Molecule 2	
Os(1)–P(1)	2.300(2)	Os(2)–P(3)	2.292(2)
Os(1)–P(2)	2.305(2)	Os(2)–P(4)	2.280(2)
Os(1)–S(1)	2.475(2)	Os(2)–S(5)	2.390(2)
Os(1)–S(2)	2.402(2)	Os(2)–S(6)	2.479(2)
Os(1)–S(3)	2.396(2)	Os(2)–S(7)	2.470(2)
Os(1)–S(4)	2.475(2)	Os(2)–S(8)	2.396(2)
P(1)–Os(1)–S(1)	87.4(1)	P(3)–Os(2)–S(5)	95.9(1)
P(1)–Os(1)–S(2)	93.8(1)	P(3)–Os(2)–S(6)	85.2(1)
P(1)–Os(1)–S(3)	96.5(1)	P(3)–Os(2)–S(7)	161.5(1)
P(1)–Os(1)–S(4)	164.0(1)	P(3)–Os(2)–S(8)	94.1(1)
P(2)–Os(1)–S(1)	163.4(1)	P(4)–Os(2)–S(5)	93.7(1)
P(2)–Os(1)–S(2)	96.1(1)	P(4)–Os(2)–S(6)	163.1(1)
P(2)–Os(1)–S(3)	93.9(1)	P(4)–Os(2)–S(7)	88.9(1)
P(2)–Os(1)–S(4)	86.9(1)	P(4)–Os(2)–S(8)	95.0(1)
S(1)–Os(1)–S(2)	70.7(1)	S(5)–Os(2)–S(6)	70.7(1)
S(1)–Os(1)–S(3)	96.9(1)	S(5)–Os(2)–S(7)	97.0(1)
S(1)–Os(1)–S(4)	84.8(1)	S(5)–Os(2)–S(8)	164.8(1)
S(2)–Os(1)–S(3)	163.5(1)	S(6)–Os(2)–S(7)	86.7(1)
S(2)–Os(1)–S(4)	96.8(1)	S(6)–Os(2)–S(8)	98.9(1)
S(3)–Os(1)–S(4)	70.7(1)	S(7)–Os(2)–S(8)	70.7(1)
P(1)–Os(1)–P(2)	103.9(1)	P(3)–Os(2)–P(4)	103.4(1)

in both the L ligands while in molecule 2 the configuration is *syn* in one and *anti* in the other. In both *trans*-$[OsL_2(PPh_3)_2]$ and *trans*-$[OsL_2(PPh_3)_2]PF_6$ the metal atoms lie on crystallographic inversion centres and the terminal methyl groups adopt *syn* configuration. The PF_6^- ion of the trivalent complex lies on a crystallographic two-fold axis.

In all the three complexes the chelate rings are nearly ideally planar and indeed the non-hydrogen atoms of each OsL fragment ignoring the terminal methyl carbons constitute excellent planes (mean deviation 0.03–0.06 Å). The OsS_4P_2 coordination spheres generally display large angular deviations from idealised octahedral geometry, one common reason for this being the very acute chelate bite angles. In *cis*-$[OsL_2(PPh_3)_2]$ an additional distorting factor is the steric repulsion[17,18] between the two *cis*-phosphine ligands. This is reflected in the structural data in two ways: considerable obtuseness of the P–Os–P angles (≈104°) and staggering

Table 3 Selected bond distances (Å) and angles (°) for *trans*-$[OsL_2(PPh_3)_2]$ and *trans*-$[OsL_2(PPh_3)_2]PF_6$

	trans-$[OsL_2(PPh_3)_2]$	*trans*-$[OsL_2(PPh_3)_2]PF_6$
Os–P(1)	2.337(8)	2.449(2)
Os–S(1)	2.427(5)	2.384(2)
Os–S(2)	2.416(8)	2.378(2)
C(1)–S(1)	1.693(24)	1.727(8)
C(1)–S(2)	1.774(25)	1.739(8)
C(1)–N(1)	1.302(30)	1.306(11)
P(1)–Os–S(1)	85.5(2)	83.8(1)
P(1)–Os–S(2)	93.0(3)	93.1(1)
S(1)–Os–S(2)	70.9(2)	72.5(1)
S(1)–C(1)–S(2)	108.2(12)	108.7(5)

Table 4 Reduction potentials * and equilibrium constants at 303 K

$E_{\frac{1}{2}}(cis)$/V	$E_{\frac{1}{2}}(trans)$/V	K^{II}	K^{III}
0.05	−0.23	6.03	7.51×10^3

* Conditions: solvent, dichloromethane; supporting electrolyte, NEt_4ClO_4 (0.1 mol dm^{-3}); working electrode, platinum; reference electrode, SCE; solute concentration, $\approx 10^{-3}$ mol dm^{-3}. $E_{\frac{1}{2}} = 0.5(E_{pa} + E_{pc})$, where E_{pa} and E_{pc} are anodic and cathodic peak potentials, respectively; scan rate, 50 mV s^{-1}.

(viewed along P–P axis) of the three carbon atoms directly bonded to one P atom with respect to those bonded to the other P atom (Fig. 5).

The Os–S lengths in the *trans*-$[OsL_2(PPh_3)_2]$ and *trans*-$[OsL_2(PPh_3)_2]^+$ follow the order $Os^{II} > Os^{III}$ — the average value in the former being longer by ≈0.05 Å. This is consistent with the predominantly σ-donor character of L^- which senses Os^{III} as a smaller ion than Os^{II}. In contrast the Os–P lengths follow the opposite order, $Os^{II} < Os^{III}$. The Os–P length in *trans*-$[OsL_2(PPh_3)_2]$ is shorter by ≈0.11 Å than in *trans*-$[OsL_2(PPh_3)_2]^+$. This remarkable change in the Os–P length is attributed to a large augmentation of $5d_\pi$–$3d_\pi$ back-bonding[19] in the OsP_2 fragment upon metal reduction ($Os^{III} \longrightarrow Os^{II}$).

In *cis*-$[OsL_2(PPh_3)_2]$ the Os–S distances *trans* to PPh_3 are significantly longer (*trans* effect) than the others but the average value lies close to that in the bivalent *trans* isomer. The more significant observation is that the average Os–P distance in the complex is shorter than that in the *trans*-$[OsL_2(PPh_3)_2]$ by ≈0.05 Å. This is logically attributed to the back-bonding order *cis*-$[OsL_2(PPh_3)_2]$ > *trans*-$[OsL_2(PPh_3)_2]$ arising from the fact that three and two metal d_π orbitals are available for π-acceptance in the *cis* and *trans* isomers respectively.

Geometry–Valence Selectivity.—In dichloromethane solution *trans*-$[OsL_2(PPh_3)_2]$ isomerises to the *cis* form with concomitant spectral changes (Fig. 6) until equilibrium is reached. Equilibrium constant data are listed in Table 4 for the equilibria (1) and (2). The constant K^{II} was determined spectro-

$$trans\text{-}[OsL_2(PPh_3)_2] \overset{K^{II}}{\rightleftharpoons} cis\text{-}[OsL_2(PPh_3)_2] \quad (1)$$

$$K^{II} = [cis\text{-}OsL_2(PPh_3)_2]/[trans\text{-}OsL_2(PPh_3)_2]$$

$$cis\text{-}[OsL_2(PPh_3)_2]^+ \overset{K^{III}}{\rightleftharpoons} trans\text{-}[OsL_2(PPh_3)_2]^+ \quad (2)$$

$$K^{III} = [trans\text{-}OsL_2(PPh_3)_2{}^+]/[cis\text{-}OsL_2(PPh_3)_2{}^+]$$

photometrically. For the trivalent state the equilibrium (2) lies far in favour of the *trans* form. The value of K^{III} was

Table 5 Rate constants and activation parameters in dichloromethane for $[OsL_2(PPh_3)_2]$

trans-$[OsL_2(PPh_3)_2]$ ⟶ *cis*-$[OsL_2(PPh_3)_2]$				*cis*-$[OsL_2(PPh_3)_2]^+$ ⟶ *trans*-$[OsL_2(PPh_3)_2]^+$			
T/K	10^4k^{II}/s^{-1}	$\Delta H^{\ddagger}$/kJ mol^{-1}	$\Delta S^{\ddagger}$/J K^{-1} mol^{-1}	T/K	10^2k^{III}/s^{-1}	$\Delta H^{\ddagger}$/kJ mol^{-1}	$\Delta S^{\ddagger}$/J K^{-1} mol^{-1}
298	6.7	72.7	−63.5	293	3.8	55.8	−82.5
303	10.6			298	6.1		
308	17.8			303	8.5		

Table 6 Experimental data for the crystallographic analyses

Compound	*cis*-$[OsL_2(PPh_3)_2]$	*trans*-$[OsL_2(PPh_3)_2]$	*trans*-$[OsL_2(PPh_3)_2]PF_6$
Formula	$C_{46}H_{50}N_2OsP_2S_4$	$C_{46}H_{50}N_2OsP_2S_4$	$C_{46}H_{50}F_6N_2OsP_3S_4$
M	1011.3	1011.3	1156.2
Crystal size (mm)	0.24 × 0.36 × 0.18	0.24 × 0.18 × 0.30	0.20 × 0.12 × 0.24
Space group	$P\bar{1}$	$P2_1/a$	$C2/c$
a/Å	11.827(4)	11.650(4)	24.823(11)
b/Å	19.287(6)	15.7461(10)	11.240(4)
c/Å	20.892(6)	11.8095(8)	18.156(6)
α/°	94.45(3)	90	90
β/°	104.22(3)	94.239(16)	108.74(3)
γ/°	100.95(3)	90	90
U/Å^3	4497(2)	2160.4(7)	4797(3)
Z	4	2	4
D_c/g dm^{-3}	1.494	1.555	1.601
μ(Mo-Kα) cm^{-1}	31.27	32.47	29.84
F(000)	2040	1020	2316
2θ range/°	2–50	2–55	2–52
Total no. of reflections	16 745	4144	5324
No. of unique reflections	15 755	3770	4709
No. of observed reflections [$I > 3\sigma(I)$]	10 635	1457	3139
Transmission factor[a]	0.875	0.893	0.926
g in $w = 1/[\sigma^2(F_o) + gF_o^2]$	0.0006	0.0005	0.0003
Data-to-parameter ratio	16.8	9.0	11.0
Final R	0.0383	0.0639	0.0385
Final R'[b]	0.4070	0.0740	0.0445
Goodness of fit[b]	0.89	0.95	1.43
Largest difference peak e Å^{-3}	0.79	0.82	0.76

[a] Maximum transmission factor is normalized to 1.0. [b] $R' = [\Sigma w(|F_o| - |F_c|)^2/\Sigma w|F_o|^2]^{\frac{1}{2}}$; goodness of fit = $[\Sigma w(|F_o| - |F_c|^2)/(N_o - N_p)]^{\frac{1}{2}}$, where N_o, N_p = numbers of observations and parameters.

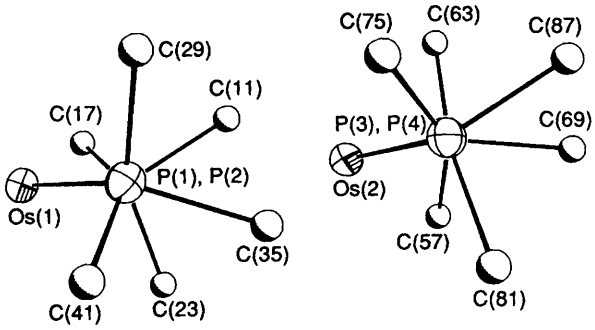

Fig. 5 The PC_3 fragments of *cis*-$[OsL_2(PPh_3)_2]$ viewed along the P–P axis

estimated electrochemically. The bivalent state displays a good degree of preference for the *cis* form (85% at equilibrium). In contrast, the trivalent state very strongly disfavours the *cis* geometry (≈0.002% at equilibrium).

These findings are consistent with the structural results. The *cis*-$[OsL_2(PPh_3)_2]$ isomer has the strong advantage of maximised Os–P back-bonding and the disadvantage of $PPh_3 \cdots PPh_3$ repulsion. In *trans*-$[OsL_2(PPh_3)_2]$ the latter is absent but the back-bonding is also weaker. The two opposing factors combine to afford an equilibrium situation in which both isomers are measurably present but the *cis* form predominates. This result underlines the great importance of back-bonding in Os^{II}–PPh_3 chemistry. For trivalent osmium back-bonding (if present) is too weak significantly to influence isomer stability. Consequently the steric factor becomes fully controlling and the *cis* isomer is greatly destabilised leading to a negligible equilibrium concentration. We thus have the inequality $K^{III} \gg K^{II}$. The *cis*-$[OsL_2(PPh_3)_2]^+$ isomer can be observed in cyclic voltammetric experiments (see below) but it has eluded isolation due to fast and virtually complete isomerisation to the *trans* form.

The rates of isomerisations (3) and (4) have been determined

$$trans\text{-}[OsL_2(PPh_3)_2] \xrightarrow{k^{II}} cis\text{-}[OsL_2(PPh_3)_2] \quad (3)$$

$$cis\text{-}[OsL_2(PPh_3)_2]^+ \xrightarrow{k^{III}} trans\text{-}[OsL_2(PPh_3)_2]^+ \quad (4)$$

using spectrophotometric and voltammetric[20] methods respectively. Both reactions are first order in nature. Rate-constant and activation parameters are listed in Table 5. The inequality $k^{III} \gg k^{II}$ is not unexpected since trivalent and bivalent complexes have d^5 and d^6 configurations respectively.[21] The isomerisations have relatively large negative entropies of activation suggesting twist mechanisms.[22]

Reduction Potentials.—The stereoretentive redox processes, equations (5) and (6), interconverting trivalent and bivalent

Table 7 Atomic coordinates ($\times 10^4$) for *cis*-$[OsL_2(PPh_3)_2]$

Atom	*x*	*y*	*z*	Atom	*x*	*y*	*z*
Os(1)	2 265(1)	2 763(1)	8 622(1)	Os(2)	2 382(1)	7 211(1)	6 040(1)
P(1)	391(2)	2 421(1)	8 778(1)	P(3)	2 001(2)	7 550(1)	7 028(1)
P(2)	2 998(2)	1 738(1)	8 666(1)	P(4)	4 414(2)	7 510(1)	6 278(1)
S(1)	2 051(2)	4 010(1)	8 798(1)	S(5)	2 337(2)	5 995(1)	6 206(1)
S(2)	3 175(2)	3 241(1)	9 769(1)	S(6)	282(2)	6 532(1)	5 714(1)
S(3)	1 641(2)	2 616(1)	7 429(1)	S(7)	2 298(2)	7 065(1)	4 843(1)
S(4)	3 970(2)	3 275(1)	8 190(1)	S(8)	2 080(2)	8 288(1)	5 593(1)
N(1)	3 106(9)	4 612(4)	10 066(4)	N(3)	158(6)	5 130(3)	5 857(3)
N(2)	3 295(8)	3 240(5)	6 846(4)	N(4)	1 774(7)	8 209(4)	4 265(3)
C(1)	2 811(8)	4 047(4)	9 612(4)	C(47)	812(7)	5 790(4)	5 923(3)
C(2)	3 608(19)	4 568(9)	10 777(8)	C(48)	−1 148(8)	4 982(5)	5 600(4)
C(3)	4 747(25)	4 761(12)	10 893(12)	C(49)	−1 810(9)	4 861(7)	6 118(6)
C(4)	2 783(12)	5 284(5)	9 896(6)	C(50)	694(9)	4 527(4)	6 030(5)
C(5)	1 563(15)	5 332(8)	9 950(9)	C(51)	1 020(10)	4 460(5)	6 760(5)
C(6)	3 034(7)	3 065(4)	7 404(4)	C(52)	2 012(6)	7 901(4)	4 818(4)
C(7)	4 475(11)	3 668(9)	6 869(7)	C(53)	1 573(11)	8 926(6)	4 296(6)
C(8)	4 499(15)	4 446(11)	6 881(10)	C(54)	290(14)	8 955(9)	4 192(9)
C(9)	2 455(12)	3 024(7)	6 196(5)	C(55)	1 723(9)	7 852(6)	3 617(4)
C(10)	2 663(18)	2 396(9)	5 829(8)	C(56)	2 883(12)	8 047(8)	3 435(6)
C(11)	−563(7)	1 544(4)	8 406(4)	C(57)	769(7)	8 039(4)	6 959(4)
C(12)	−1 579(9)	1 244(5)	8 596(5)	C(58)	610(9)	8 394(5)	7 521(5)
C(13)	−2 330(10)	611(6)	8 246(6)	C(59)	−292(11)	8 746(6)	7 497(6)
C(14)	−2 077(9)	272(6)	7 715(5)	C(60)	−1 069(11)	8 769(6)	6 901(6)
C(15)	−1 099(9)	563(5)	7 517(5)	C(61)	−931(9)	8 433(5)	6 314(5)
C(16)	−341(7)	1 197(4)	7 863(4)	C(62)	−24(8)	8 068(5)	6 355(4)
C(17)	−716(7)	2 960(4)	8 428(4)	C(63)	1 477(7)	6 815(4)	7 485(4)
C(18)	−579(8)	3 357(4)	7 917(4)	C(64)	2 241(10)	6 429(5)	7 799(5)
C(19)	−1 420(9)	3 749(5)	7 667(5)	C(65)	1 864(11)	5 833(6)	8 109(6)
C(20)	−2 382(10)	3 749(6)	7 906(5)	C(66)	705(11)	5 659(7)	8 091(6)
C(21)	−2 564(11)	3 340(6)	8 401(6)	C(67)	−95(11)	6 020(6)	7 780(6)
C(22)	−1 729(8)	2 948(5)	8 659(5)	C(68)	265(9)	6 612(5)	7 456(5)
C(23)	278(7)	2 477(4)	9 637(4)	C(69)	3 130(7)	8 195(4)	7 681(4)
C(24)	356(8)	3 146(5)	9 984(5)	C(70)	3 659(8)	8 059(5)	8 321(5)
C(25)	363(9)	3 219(6)	10 652(5)	C(71)	4 494(9)	8 597(5)	8 777(5)
C(26)	302(9)	2 625(5)	10 983(5)	C(72)	4 813(9)	9 261(5)	8 596(5)
C(27)	240(8)	1 979(5)	10 660(5)	C(73)	4 292(8)	9 399(5)	7 970(5)
C(28)	222(8)	1 894(5)	9 993(4)	C(74)	3 467(8)	8 870(5)	7 517(5)
C(29)	3 103(7)	1 280(4)	7 884(4)	C(75)	5 169(7)	6 886(4)	5 902(4)
C(30)	4 123(10)	1 479(6)	7 667(5)	C(76)	6 405(9)	7 009(5)	6 089(5)
C(31)	4 189(12)	1 132(6)	7 051(6)	C(77)	7 016(11)	6 610(6)	5 763(6)
C(32)	3 281(11)	635(6)	6 676(7)	C(78)	6 388(10)	6 078(6)	5 259(5)
C(33)	2 263(10)	433(6)	6 868(6)	C(79)	5 155(9)	5 933(5)	5 075(5)
C(34)	2 182(9)	771(5)	7 463(5)	C(80)	4 550(8)	6 336(5)	5 398(4)
C(35)	2 389(7)	1 004(4)	9 084(4)	C(81)	5 067(7)	8 327(4)	5 976(4)
C(36)	2 188(10)	282(6)	8 845(6)	C(82)	5 405(9)	8 280(6)	5 400(5)
C(37)	1 866(11)	−239(7)	9 240(6)	C(83)	5 809(12)	8 897(7)	5 138(7)
C(38)	1 708(10)	−19(6)	9 856(6)	C(84)	5 898(12)	9 551(7)	5 476(7)
C(39)	2 005(10)	674(6)	10 111(6)	C(85)	5 570(10)	9 610(6)	6 034(6)
C(40)	2 339(9)	1 181(5)	9 714(5)	C(86)	5 118(9)	8 992(5)	6 300(5)
C(41)	4 579(7)	1 838(4)	9 154(4)	C(87)	5 285(8)	7 563(4)	7 131(4)
C(42)	5 050(8)	1 233(5)	9 230(5)	C(88)	5 109(10)	6 947(6)	7 446(6)
C(43)	6 207(9)	1 282(5)	9 617(5)	C(89)	5 761(12)	6 926(7)	8 105(7)
C(44)	6 899(10)	1 931(6)	9 928(5)	C(90)	6 627(13)	7 513(7)	8 430(7)
C(45)	6 466(9)	2 523(5)	9 851(5)	C(91)	6 842(12)	8 093(7)	8 141(7)
C(46)	5 302(8)	2 492(5)	9 458(4)	C(92)	6 184(9)	8 125(6)	7 495(5)

Table 8 Atomic coordinates ($\times 10^4$) for *trans*-$[OsL_2(PPh_3)_2]$

Atom	*x*	*y*	*z*	Atom	*x*	*y*	*z*
Os	0	0	0	C(10)	−2769(24)	1198(16)	−3288(21)
P(1)	332(7)	950(5)	−1461(7)	C(11)	−1910(22)	1200(16)	−2469(22)
S(1)	1947(5)	339(3)	734(5)	C(12)	1649(18)	809(13)	−2181(17)
S(2)	−68(7)	1119(5)	1393(7)	C(13)	2311(16)	86(21)	−2058(15)
N(1)	2041(16)	1639(14)	2239(16)	C(14)	3281(17)	−26(29)	−2646(16)
C(1)	1457(20)	1100(14)	1589(19)	C(15)	3637(24)	636(16)	−3333(22)
C(2)	3318(20)	1586(15)	2345(20)	C(16)	3031(23)	1387(17)	−3442(21)
C(3)	3799(31)	1154(22)	3303(27)	C(17)	2035(20)	1477(15)	−2869(18)
C(4)	1484(23)	2296(16)	2914(21)	C(18)	492(19)	2090(13)	−1009(18)
C(5)	1042(30)	1962(21)	3976(26)	C(19)	−416(19)	2673(13)	−1096(17)
C(6)	−773(19)	1001(14)	−2661(18)	C(20)	−262(24)	3476(17)	−611(22)
C(7)	−566(24)	808(16)	−3757(21)	C(21)	781(21)	3726(16)	−101(20)
C(8)	−1432(27)	823(19)	−4628(26)	C(22)	1664(22)	3152(15)	9(21)
C(9)	−2542(29)	1047(20)	−4379(28)	C(23)	1526(21)	2351(15)	−466(19)

$$trans\text{-}[OsL_2(PPh_3)_2]^+ + e \rightleftharpoons trans\text{-}[OsL_2(PPh_3)_2] \quad (5)$$

$$cis\text{-}[OsL_2(PPh_3)_2]^+ + e \rightleftharpoons cis\text{-}[OsL_2(PPh_3)_2] \quad (6)$$

states can be observed by cyclic voltammetry (Fig. 7). The $E_{\frac{1}{2}}$ of the *trans* couple is significantly lower than that of the *cis* couple (Table 4). This is expected since the redox electron is a $5d_\pi$ electron which is stabilised better in the *cis* than in the *trans* isomer (back-bonding).

The *trans* couple can be observed using fresh solutions of either the bivalent or the trivalent *trans* isomer. No isomerisation (bivalent *trans* ⟶ *cis*) is observed on the cyclic voltammetric time-scale in the temperature range 273–298 K. The bivalent *cis* complex gives rise to the *cis* couple alone at 273 K. In warmer solutions, *cis*-$[OsL_2(PPh_3)_2]^+$ produced in the anodic scan isomerises sufficiently rapidly to the *trans* form to make the *trans* couple observable on scan reversal (Fig. 7). Coulometrically oxidised [at 0.3 V *vs.* saturated calomel electrode (SCE)] solutions of *cis*-$[OsL_2(PPh_3)_2]$ are found to contain only *trans*-$[OsL_2(PPh_3)_2]^+$ due to rapid isomerisation following stereoretentive oxidation.

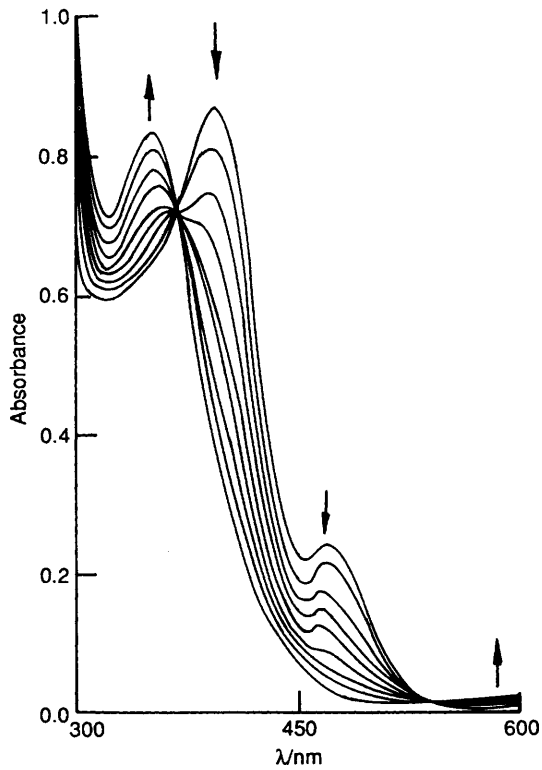

Fig. 6 Time evolution of the electronic spectrum of *trans*-$[OsL_2(PPh_3)_2]$ isomerising to the *cis* form in dichloromethane at 303 K. The arrows indicate increase and decrease in band intensities as the reaction proceeds

Some General Comments on the OsS_4P_2 *Systems.*—In our study of isomer preference of oxidation states we chose osmium with the hope that isomerisation rates will be slow enough to permit isolation and structural characterisation of metastable isomers. This has been realised in the case of *trans*-$[OsL_2(PPh_3)_2]$. The present work constitute the concluding part of our general programme on OsS_4P_2 species—dithiocarbonates,[8] **2** and trithiocarbonates,[9] **3** having been described earlier. The OsS_4P_2 co-ordination spheres of the three systems have served as excellent models for probing isomer–

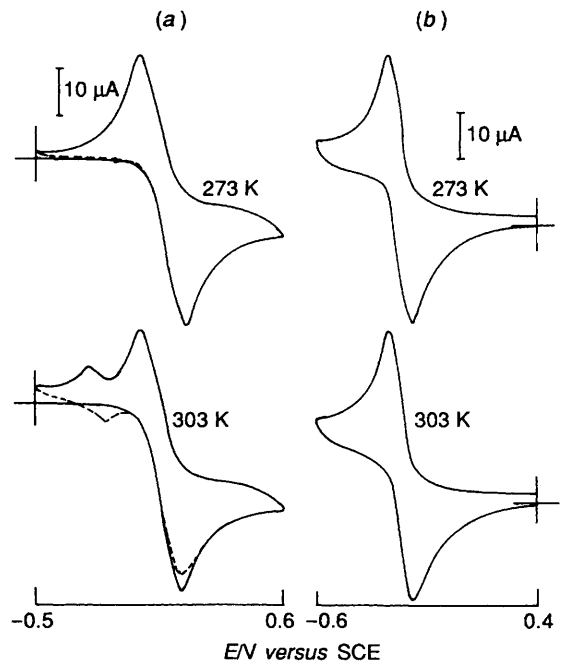

Fig. 7 Variable-temperature cyclic voltammograms (scan rate 50 mV s^{-1}) of $\approx 10^{-3}$ mol dm^{-3} solutions of (*a*) *cis*-$[OsL_2(PPh_3)_2]$[first cycle (——), second cycle (– – –)] and (*b*) *trans*-$[OsL_2(PPh_3)_2]PF_6$ in dichloromethane

Table 9 Atomic coordinates ($\times 10^4$) for *trans*-$[OsL_2(PPh_3)_2]PF_6$

Atom	*x*	*y*	*z*	Atom	*x*	*y*	*z*
Os	2500	2500	0	C(12)	1368(3)	1511(6)	−1762(4)
S(1)	2276(1)	1937(2)	1133(1)	C(13)	865(4)	1995(8)	−2220(5)
S(2)	2035(1)	4143(2)	361(1)	C(14)	704(4)	1888(9)	−3018(5)
P(1)	1603(1)	1500(2)	−687(1)	C(15)	1036(4)	1279(8)	−3364(5)
P(2)	0	4394(3)	2500	C(16)	1542(4)	802(8)	−2909(5)
N(1)	1615(3)	3587(6)	1521(3)	C(17)	1702(3)	911(7)	−2114(4)
C(1)	1924(3)	3273(6)	1091(4)	C(18)	1577(3)	−102(6)	−522(4)
C(2)	1519(4)	2745(8)	2094(5)	C(19)	1108(3)	−736(7)	−1014(5)
C(3)	1950(5)	2837(11)	2871(6)	C(20)	1049(4)	−1947(8)	−890(5)
C(4)	1357(4)	4775(8)	1461(5)	C(21)	1443(4)	−2517(9)	−301(5)
C(5)	1733(5)	5653(10)	1943(8)	C(22)	1898(4)	−1909(8)	197(5)
C(6)	997(3)	2052(7)	−413(4)	C(23)	1968(3)	−699(6)	93(4)
C(7)	781(3)	3192(7)	−616(4)	F(1)	659(3)	4379(7)	2944(5)
C(8)	347(3)	3603(8)	−364(5)	F(2)	0	2934(20)	2500
C(9)	128(4)	2933(9)	85(5)	F(3)	0	5803(16)	2500
C(10)	340(4)	1796(10)	307(5)	F(4)	96(5)	4254(10)	1705(7)
C(11)	776(3)	1357(8)	54(5)				

valence selectivity in terms of bond parameters. To our knowledge **1**–**3** are the only osmium species where the remarkable changes in back-bonding abilities in going from the bivalent to the trivalent states and from the *cis* to the *trans* geometry of the bivalent state have been demonstrated through structure determination of relevant isomers.

The isomer preferences of **1**, **2** and **3** are very similar and corresponding bond parameters generally lie close to one another. For the bivalent state, the average Os–P length of **1** is slightly shorter (by ≈0.02 Å) than those of the corresponding isomers[8,9] of **2** and **3**; also the P–Os–P angle is more obtuse (by ≈2.9°) in *cis*-**1**. These are indicative that back-bonding may be somewhat stronger in the bivalent diethyldithiocarbamate complexes. Among the three concerned sulfur ligands, diethyldithiocarbamate has more negative charge on the sulfur atoms [larger contribution of canonical form $=C(S^-)S^-$].[23] A higher degree of σ transfer of negative charge to the metal is expected to strengthen back donation *via* σ–π synergism.

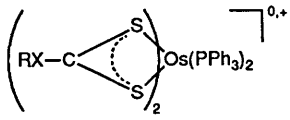

2 X = O
3 X = S

Experimental

Materials.—Osmium tetraoxide obtained from Arora-Matthey Calcutta, India was treated with HBr to afford $[NH_4]_2[OsBr_6]$[24] which was converted[25] to $[Os(PPh_3)_3Br_2]$. Sodium diethyldithiocarbamate (NaL) was purchased from Aldrich. The preparation of tetraethylammonium perchlorate and the purification of solvents for electrochemical and spectroscopic work were as done before.[8] All other chemicals and solvents were of reagent grade and used without further purification.

Physical Measurements.—The UV/VIS/NIR spectra were recorded on a Hitachi 330 spectrophotometer and infrared (4000–300 cm^{-1}) spectra on a Perkin Elmer 783 spectrophotometer. The magnetic susceptibility was measured on a PAR 155 vibrating-sample magnetometer fitted with a Walker Scientific L75FBAL magnet. X-Band EPR spectra were recorded on a Varian E-109C spectrometer fitted with a quartz Dewar flask for measurements at 77 K (liquid nitrogen) and calibrated with respect to diphenylpicrylhydrazyl (dpph) (g = 2.0037). Electrochemical measurements were done by using a PAR model 370–4 electrochemistry system as described elsewhere.[8] All experiments were performed under a dinitrogen atmosphere and reported potentials are uncorrected for the junction contribution. Haake model-F3K and model-D8G digital cryostats and circulators connected to appropriate jacketed cells were used for low-temperature measurements. Solution electrical conductivity was measured by using a Philips PR 9500 bridge. Microanalytical data (C, H and N) were obtained with the use of a Perkin Elmer model 240C elemental analyser.

Preparations.—cis-*Bis(diethyldithiocarbamato)bis(triphenylphosphine)osmium*(II), *cis*-$[OsL_2(PPh_3)_2]$. To a warm solution of $[Os(PPh_3)_3Br_2]$ (200 mg, 0.18 mmol) in ethanol (30 cm^3) was added hydrated sodium diethyldithiocarbamate (NaL) (100 mg, 0.44 mmol). The mixture was refluxed for 1 h. Upon cooling a yellow microcrystalline solid separated which was collected by filtration, washed thoroughly with water and ethanol, and dried *in vacuo* over P_4O_{10}, yield 92%.

trans-*Bis(diethyldithiocarbamato)bis(triphenylphosphine)osmium*(III) *hexafluorophosphate*, *trans*-$[OsL_2(PPh_3)_2]PF_6$. To a solution of pure *cis*-$[OsL_2(PPh_3)_2]$ (100 mg, 0.098 mmol) in dichloromethane–acetonitrile (2:3, 25 cm^3) was added ammonium cerium(IV) sulfate (95 mg, 0.15 mmol) dissolved in water (15 cm^3). The mixture was stirred magnetically for 15 min during which time the colour of the solution became deep green. The reaction mixture was then filtered, the filtrate concentrated to 10 cm^3 under reduced pressure and a saturated aqueous solution of NH_4PF_6 (10 cm^3) added. The deep green solid thus obtained was collected by filtration, washed with water, and dried *in vacuo* over P_4O_{10}, yield 95%.

trans-*Bis(diethyldithiocarbamato)bis(triphenylphosphine)osmium*(II), *trans*-$[OsL_2(PPh_3)_2]$. The complex *trans*-$[OsL_2(PPh_3)_2]PF_6$ (100 mg, 0.086 mmol) was dissolved in acetonitrile (15 cm^3) and stirred magnetically at 273 K under a stream of nitrogen. Hydrazine hydrate (35 mg, 0.7 mmol) in acetonitrile (5 cm^3) was added dropwise. The green solution immediately changed to orange-yellow and a solid separated out. Stirring was continued for 10 min. The orange-yellow solid thus obtained was collected by filtration. The mass was washed with water and acetonitrile and dried *in vacuo* over P_4O_{10}, yield 95%.

Determination of Equilibrium Constants and Rates.—The constant K^{II} was determined (303 K) by monitoring the residual intensity of the 475 nm spectral band of equilibrated (10 h) solutions of *trans*-$[OsL_2(PPh_3)_2]$. The band is characteristic of the *trans* isomer (Fig. 6). The constant K^{III} was estimated from the values[8,9] of K^{II}, $E_{\frac{1}{2}}(cis)$ and $E_{\frac{1}{2}}(trans)$ using equation (7) which is readily derived with the help of

$$K^{II}K^{III} = \exp\{F/RT[E_{\frac{1}{2}}(cis) - E_{\frac{1}{2}}(trans)]\} \quad (7)$$

a thermodynamic cycle interlinking the equilibria (1), (2), (5) and (6).

The rate constant k^{II} was determined by following the decrease in the intensity of the spectral band at 475 nm (characteristic of *trans* form) with time (Fig. 6). The rate constant k^{III} was estimated from electrochemical data using a reported method.[20]

X-*Ray Structure Determinations.*—Single crystals were grown (at 298 K for *cis*-$[OsL_2(PPh_3)_2]$ *and* *trans*-$[OsL_2(PPh_3)_2]PF_6$, and at 273 K for *trans*-$[OsL_2(PPh_3)_2]$) by slow diffusion of hexane into dichloromethane solutions of the compounds. Selected crystal data and data collection parameters are given in Table 6. Data were collected on a Nicolet R3m/V diffractometer using graphite-monochromated Mo-Kα radiation (λ = 0.710 73 Å) and were corrected for Lorentz and polarisation factors. Two standard reflections after each 98 reflections measured for all three cases showed no significant variations. An empirical absorption correction was done on each set of data on the basis of azimuthal scans.[26]

All three structures were solved by using the heavy-atom method, the position of the metal atoms being determined from Patterson maps and the remaining non-hydrogen atoms by successive Fourier difference syntheses. Non-hydrogen atoms except for the phenyl carbon atoms in the cases of *cis*-$[OsL_2(PPh_3)_2]$ and *trans*-$[OsL_2(PPh_3)_2]$ were refined anisotropically. Hydrogen atoms were included at their calculated positions with a fixed isotropic thermal parameter of 0.08 $Å^2$ in the final cycle of refinement. Final residuals and the maximum residual electron densities in the final ΔF map in the three cases are as given in Table 6. Atomic coordinates for the non-hydrogen atoms are collected in Tables 7–9. All computations regarding data reduction, structure solution and refinement were carried out on a MicroVAX II computer using the SHELXTL-PLUS[27] program package.

Additional material available from the Cambridge Crystallographic Data Centre comprises H-atom coordinates, thermal parameters and remaining bond lengths and angles.

Acknowledgements

Crystallography was done at the National Single Crystal Diffractometer Facility, Department of Inorganic Chemistry, Indian Association for the Cultivation of Science. Financial support received from the Department of Science and Technology, New Delhi, India and the Council of Scientific and Industrial Research, New Delhi, India is acknowledged.

References

1 W. E. Geiger, *Prog. Inorg. Chem.*, 1985, **33**, 275; D. H. Evans and K. M. O'Connell, in *Electroanalytical Chemistry. A Series of Advances*, ed. A. J. Bard, Marcel Dekker, New York, 1986, vol. 14, p. 113.
2 J. Lewis and R. Whyman, *J. Chem. Soc.*, 1965, 5486; P. F. Crossing and M. R. Snow, *J. Chem. Soc. A*, 1971, 610.
3 A. M. Bond, R. Colton and J. E. Kevekordes, *Inorg. Chem.*, 1986, **25**, 749; A. M. Bond, R. Colton, J. E. Kevekordes and P. Panagiotidon, *Inorg. Chem.*, 1987, **26**, 1430 and refs. therein.
4 F. Bombin, G. A. Carriedo, J. A. Miguel and V. Riera, *J. Chem. Soc., Dalton Trans.*, 1981, 2049; K. A. Conner and R. A. Walton, *Inorg. Chem.*, 1986, **25**, 4422; A. Vallat, M. Person, L. Roullier and E. Laviron, *Inorg. Chem.*, 1987, **26**, 332; N. G. Connelly, K. A. Hassard, B. J. Dunne, A. G. Orpen, S. J. Raven, G. A. Carriedo and V. Riera, *J. Chem. Soc., Dalton Trans.*, 1988, 1623.
5 B. P. Sullivan and T. J. Meyer, *Inorg. Chem.*, 1982, **21**, 1037; N. Bag, G. K. Lahiri and A. Chakravorty, *J. Chem. Soc., Dalton Trans.*, 1990, 1557; A. Pramanik, N. Bag, G. K. Lahiri and A. Chakravorty, *J. Chem. Soc., Dalton Trans.*, 1990, 3823.
6 R. A. Rader and D. R. McMillin, *Inorg. Chem.*, 1979, **18**, 545; A. M. Bond, F. R. Keene, N. W. Rumble, G. H. Searle and M. R. Snow, *Inorg. Chem.*, 1978, **17**, 2847; A. M. Bond, T. W. Hambley and M. R. Snow, *Inorg. Chem.*, 1985, **24**, 1920.
7 D. Ray and A. Chakravorty, *Inorg. Chem.*, 1988, **27**, 3292; P. Basu, S. Pal and A. Chakravorty, *J. Chem. Soc., Chem. Commun.*, 1989, 977; P. Basu, S. B. Choudhury, S. Pal and A. Chakravorty, *Inorg. Chem.*, 1989, **28**, 2680; P. Basu and A. Chakravorty, *J. Chem. Soc., Chem. Commun.*, 1992, 809.
8 A. Pramanik, N. Bag, D. Ray, G. K. Lahiri and A. Chakravorty, *Inorg. Chem.*, 1991, **30**, 410.
9 A. Pramanik, N. Bag, D. Ray, G. K. Lahiri and A. Chakravorty, *J. Chem. Soc., Chem. Commun.*, 1991, 139; A. Pramanik, N. Bag, G. K. Lahiri and A. Chakravorty, *J. Chem. Soc., Dalton Trans.*, 1992, 101.
10 P. B. Critchlow and S. D. Robinson, *J. Chem. Soc., Dalton Trans.*, 1975, 1367.
11 G. K. Lahiri, S. Bhattacharya, B. K. Ghosh and A. Chakravorty, *Inorg. Chem.*, 1987, **26**, 4324; G. K. Lahiri, S. Bhattacharya, M. Mukherjee, A. K. Mukherjee and A. Chakravorty, *Inorg. Chem.*, 1987, **26**, 3359.
12 B. Bleaney and M. C. M. O'Brien, *Proc. Phys. Soc. London, Sect. B*, 1956, **69**, 1216; J. S. Griffith, *The Theory of Transitional Metal Ions*, Cambridge University Press, London, 1961, p. 364.
13 S. Sakaki, N. Hagiwara, Y. Yanase and A. Ohyoshi, *J. Phys. Chem.*, 1978, **82**, 1917; A. Hudson and M. J. Kennedy, *J. Chem. Soc. A*, 1969, 1116.
14 D. Coucouvanis, *Prog. Inorg. Chem.*, 1979, **26**, 301.
15 K. W. Given and L. H. Pignolet, *Inorg. Chem.*, 1977, **16**, 2982; L. J. Maheu and L. H. Pignolet, *Inorg. Chem.*, 1979, **18**, 3626.
16 M. Minelli, M. R. Carson, D. W. Whisenhunt, jun. and J. L. Hubbard, *Inorg. Chem.*, 1990, **29**, 442; M. Minelli, M. R. Carson, D. W. Whisenhunt jun. and W. Imhof, *Inorg. Chem.*, 1990, **29**, 4801.
17 C. A. Tolman, *Chem. Rev.*, 1977, **77**, 313; H. C. Clark and M. J. Hampden-Smith, *Coord. Chem. Rev.*, 1987, **79**, 229.
18 J. Powell, *J. Chem. Soc., Chem. Commun.*, 1989, 200.
19 H. Taube, *Pure Appl. Chem.*, 1979, **51**, 901; M. Sekine, W. D. Harman and H. Taube, *Inorg. Chem.*, 1988, **27**, 3604.
20 R. S. Nicholson and I. Shain, *Anal. Chem.*, 1964, **36**, 706.
21 F. Basolo and R. G. Pearson, *Mechanisms of Inorganic Reactions*, Wiley, New York, 1967.
22 N. Serpone and D. G. Bickley, *Prog. Inorg. Chem.*, 1972, **17**, 391 and refs. therein.
23 S. E. Livingstone, *Q. Rev. Chem. Soc.*, 1965, 386.
24 F. P. Dwyer and J. W. Hogarth, *Inorg. Synth.*, 1957, **5**, 204.
25 P. R. Hoffman and K. G. Caulton, *J. Am. Chem. Soc.*, 1975, **97**, 4221.
26 A. C. T. North, D. C. Philips and F. S. Mathews, *Acta Crystallogr., Sect. A*, 1968, **24**, 351.
27 G. M. Sheldrick, SHELXTL-PLUS 88, Structure Determination Software Programs, Nicolet Instrument Corporation, Madison, WI, 1988.

Received 13*th August* 1992; *Paper* 2/04387D